Available online at www.sciencedirect.com
SCIENCE DIRECT®
Journal of Solid State Chemistry 177 (2004) 1817–1828
JOURNAL OF SOLID STATE CHEMISTRY
http://elsevier.com/locate/jssc

Structure of copper-potassium hexacyanoferrate (II) and sorption mechanisms of cesium

C. Loos-Neskovic,[a] S. Ayrault,[b] V. Badillo,[c] B. Jimenez,[d] E. Garnier,[e] M. Fedoroff,[a,*] D. J. Jones,[f] and B. Merinov[f]

[a] *Centre d'Etudes de Chimie Métallurgique, CNRS, 15, rue Georges Urbain, 94407 Vitry-sur-Seine, France*
[b] *Laboratoire Pierre Süe, CEA-CNRS, CEA Saclay, 91191 Gif-sur-Yvette Cedex, France*
[c] *Centro Regional de Estudios Nucleares, Universitad Autonome de Zacatecas, 98068 Zacatecas, Zac., Mexico*
[d] *CSIC, Instituto de Quimica Organica General, Juan de la Cierva 3, 28006 Madrid, Spain*
[e] *Laboratoire d'Electrocatalyse, UMR CNRS 6530, 40 Avenue du Recteur Pineau, Université de Poitiers, 86022 Poitiers Cedex, France*
[f] *Laboratoire des Agrégats Moléculaires et Matériaux Inorganiques, UMR CNRS 5072, Université Montpellier II, Place Eugène Bataillon, 34095 Montpellier, France*

Received 21 October 2003; received in revised form 7 January 2004; accepted 16 January 2004

Abstract

A mixed potassium-copper hexacyanoferrate (II) $K_2CuFe(CN)_6$ was prepared by local growth on solid cupric sulfate in an aqueous solution of potassium hexacyanoferrate (II) and by growth in a gel. Powders having this composition and separable by filtration could not be obtained by normal precipitation from aqueous solution. This compound has a triclinic *P*-1 structure, described for the first time, and made up of non-linear –Fe–C–N–Cu-chains which form a puckered layered network. Sorption mechanisms for cesium have been studied in batch experiments including kinetics and isotherms, X-ray diffraction, infra-red spectroscopy and scanning electron microscopy. In neutral solutions the initial crystal structure is maintained and sorption proceeds through a K/Cs ion exchange. In acid solutions, even without addition of cesium, the initial structure is destroyed. The main phase formed in acidic media is $Cu_2Fe(CN)_6$. In the presence of cesium the structure is also destroyed and new solid phases are formed. All these processes have slow kinetics, the evolution of the solid being observed over a period of 6 months. This study confirms previous results, which have shown that the sorption mechanisms on hexacyanoferrates strongly depend on the composition and structure of the solid, together with the composition of the solution. Sorption mechanisms have considerable consequences on the use of these products for the decontamination of radioactive wastes.

Keywords: Cesium; Potassium copper hexacyanoferrate; Crystal structure; Sorption; Radioactive wastes

1. Introduction

The preparation of hexacyanoferrates and their application to the removal of radioactive cesium from solutions by sorption or precipitation have been studied over the past 50 years, owing to their interest for the nuclear industry [1–6]. Considerable effort has been devoted to the development and optimization of procedures using hexacyanoferrates. Concern has also been raised about the safe storage of hexacyanoferrates after extended use in the scavenging of radioactive cesium from tank waste solutions, especially when intermixed with oxidants, such as nitrate salts. The decomposition of hexacyanoferrates has been suspected to be responsible for the evolution of gases at Hanford (USA) [7]. In order to be able to better control all these processes, increased knowledge of the mechanisms involved in cesium sorption and further storage of hexacyanoferrates is needed.

Insoluble hexacyanoferrates exhibit a great variety of compositions and structures. Several compositions may be obtained and different structural arrangements observed with the same transition metal, depending on the method of preparation [8–11]. In our previous studies, we have shown that the nature of the sorption process strongly depends on the composition and crystal structure of the starting solid [12,13]. The retention of

*Corresponding author. Fax : +33-1-46-75-04-33.
E-mail address: fedoroff@glvt-cnrs.fr (M. Fedoroff).

0022-4596/$ - see front matter © 2004 Elsevier Inc. All rights reserved.
doi:10.1016/j.jssc.2004.01.018

cesium may result from a true ion exchange or may lead to a change of the crystal structure of the solid phase. These different mechanisms result in different sorption kinetics, capacities and stability of the solids, factors that have a significant impact on the choice of the most suitable compounds and experimental conditions for industrial applications.

In an effort to clarify this situation, we have previously performed a systematic study of the preparation methods, compositions, structures and sorption mechanisms of zinc and nickel hexacyanoferrates (II) [8,9], and of simple copper hexacyanoferrates (II) and (III) [10,11,13]. These compounds present a large variety of structures: a trigonal and compact structure for $Zn_2Fe^{II}(CN)_6 \cdot 2H_2O$, a zeolitic rhombohedral structure for $M^I_2Zn_3[Fe(CN)_6]_2$ (M^I = Na, K, Cs) with cavities that can host alkali metal ions and water molecules [14]. Nickel and simple copper hexacyanoferrates have structures characterized by iron vacancies in the cubic $Fm\bar{3}m$ lattice. In $Cu_2Fe^{II}(CN)_6 \cdot xH_2O$, copper atoms occupy two different crystallographic sites, atoms Cu1 in 4*b* positions linked to the CN network and atoms Cu2 in 8*b* positions. The second type of site is not present in $Cu^{II}_3[Fe^{III}(CN)_6]_2 \cdot xH_2O$ [13].

All the insoluble hexacyanoferrates studied show very high affinity and selectivity for cesium ions. $M^I_2Zn_3[Fe(CN)_6]_2$(M^I= Na, K, Cs) sorbs cesium with rapid kinetics: alkali metal ions do not belong to the Zn–Fe network and fast ion exchange Cs/M^I is observed [12]. This mechanism plays a very minor role for $Zn_2Fe^{II}(CN)_6 \cdot 2H_2O$ and $Cu_2Fe^{II}(CN)_6$. The latter compound presents the highest observed Cs uptakes. The sorption mechanism includes at least two steps: diffusion of ion pairs into the solid and formation of new solid phase [13].

Much work has been reported concerning the fixation of cesium on mixed hexacyanoferrates including copper and alkali metal ions [15–18], but these studies have often been performed with ill-defined solids. The hypothesis of ion exchange between the potassium ions in the solid and the cesium ions of the solution is generally accepted. In many publications, the mobility of alkali metal ions and their exchange within the same cubic structure are the basic phenomena assumed to take place when thin layers of copper hexacyanoferrate are submitted to cyclic voltametric experiments [19–21].

In the present study, we used $K_2CuFe(CN)_6$ obtained by a local growth method from aqueous solutions [22–24], thus allowing sorption studies on a compound of structure fundamentally different from that of the $Cu_2Fe^{II}(CN)_6$ [11,13]. Single crystals were also used in order to determine the crystal structure of $K_2CuFe(CN)_6$. The aim of this study, performed with well-characterized solids, was an understanding of the sorption mechanisms, together with an assessment of their stability and long-term evolution. For that purpose, the evolution of the solid and liquid phases throughout several months has been followed using various characterization methods.

2. Materials and methods

2.1. Preparation of potassium-copper hexacyanoferrate

2.1.1. Local growth method

This method [22–24], previously developed for the preparation of beads of definite sizes, was used for the preparation of $K_2CuFe(CN)_6$. A total of 1–25 g of solid cupric sulfate were placed in 500 mL of 0.5–0.65 M potassium hexacyanoferrate (II) solution and allowed to stand for 24 h at 21–27°C (Table 1). The particles obtained were washed with deionized water and separated by decantation. This process was repeated several times. The precipitate was allowed to dry in air and then sieved under water flow using 25, 100 and 200 μm sieves, and the various fractions dried in air at room temperature.

Table 1
Chemical compositions of potassium-copper hexacyanoferrate powders used in this study

Sample code	Yield (%)[a]	Preparation conditions				Chemical composition	K/Cu (at/at)
		$CuSO_4$ (g)	T°C	$K_4Fe^{II}(CN)_6$			
				C	V		
Cu93.5	40	1	21	0.5	0.05	$K_{1.97}Cu^{II}_{1.00}Fe(CN)_6$	1.97
Cu93.24	38	14	25	0.6	0.5	$K_{1.91}Cu^{II}_{1.05}Fe(CN)_6 \cdot 3.4H_2O$	1.82
Cu94.9	47	15	25	0.5	0.75	$K_{1.88}Cu^{II}_{1.05}Fe(CN)_6 \cdot 3.6H_2O$	1.79
Cu95.2	37	14	25	0.6	0.5	$K_{1.98}Cu^{II}_{1.18}Fe(CN)_6 \cdot 1.9H_2O$	1.68
Cu95.3	25	5	21	0.5	0.5	$K_{1.91}Cu^{II}_{1.10}Fe(CN)_6 \cdot 1.0H_2O$	1.73
Cu95.6[b]	47	5	21	0.5	0.5	$K_{2.01}Cu^{II}_{1.05}Fe(CN)_6 \cdot 1.5H_2O$	1.91
Cu00.2	12	25	27	0.65	1	$K_{1.83}Cu^{II}_{1.13}Fe(CN)_6 \cdot 3.5H_2O$	1.62

C (mol/L), V (L): concentration and volume of $K_4Fe^{II}(CN)_6$ solution.
[a] Yield of particle size >25 μm.
[b] Washed with deionized water of pH adjusted to 8 with dilute KOH solution.

2.1.2. Preparation of single crystals

Single crystals could be prepared by growth in a gel. Copper tartrate crystals were placed at the bottom of a test tube and covered with lithium or potassium metasilicate solution neutralized by 1 M acetic acid solution to $9.5 < pH < 10.5$. After setting of the metasilicate gel, a 0.15 M potassium hexacyanoferrate solution was introduced and allowed to diffuse slowly through the gel (over a period of at least 1 month). The crystals obtained were individually separated from the gel using a binocular magnifier and glass capillaries, and washed several times in a drop of water.

2.2. Characterization

2.2.1. Chemical analysis

Non-destructive neutron activation analyses (NAA) were systematically performed for the determination of Na, K, Cl, Cu and Fe using the facilities of the Pierre Süe Laboratory at Saclay. The water content was derived by difference, considering that one Fe atom is bound to six cyanide groups, and the results confirmed by thermogravimetric analyses.

The starting compounds were also analyzed for Na, K, Cu and Fe by inductively coupled plasma atomic emission spectroscopy (ICP/AES). In all 20 mg samples were dissolved in 11.6 M $HClO_4$ prior to analysis. For a complete determination of anions, some of the products were analyzed at the Service Central d'Analyses (CNRS, Vernaison, France).

2.2.2. Morphology

Scanning electron microscopy (SEM) was used to characterize the morphology. Samples were deposited on graphite plates and examined by a LEO 1530 electron microscope with Energy Dispersive X-ray spectrometry (EDX) from PGT.

2.2.3. Specific surface area measurements

Nitrogen adsorption–desorption isotherms were obtained at 77 K with a Sorptomatic Series 1800 apparatus (Carlo Erba), and the results interpreted using the BET method. Prior to measurement, the sample was outgassed at 60°C at $<10^{-4}$ Torr overnight.

2.2.4. Powder X-ray diffraction analyses

X-ray diffraction (XRD) patterns were recorded using a Siemens diffractometer D5005 in the Bragg–Brentano geometry ($\theta - \theta$), with a diffracted-beam monochromator and a 1° fixed divergence slit, with 200–400 mg of powder before and after cesium sorption. Cu$K\alpha$ X-ray radiation was used. Identification was made by reference to the JCPDS-ICDD database (release 2000).

2.2.5. Single crystal X-ray diffraction and crystal structure determination

A single crystal of dimensions $0.30 \times 0.13 \times 0.05\,mm^3$ was mounted in a Lindemann capillary tube, and the tube sealed. X-ray diffraction data were collected at 22°C on an Enraf–Nonius CAD-4 diffractometer using Mo$K\alpha$. Lattice parameters determined from preliminary oscillation experiments were refined by least-squares methods.

Of 2000 unique reflections in $h\,k\,l$ ranges $-8 \leqslant h \leqslant 8$, $-8 \leqslant k \leqslant 8, 0 \leqslant l \leqslant 8$, 374 reflections with $I \geqslant 3\sigma(I)$ were converted into moduli of structure amplitudes taking into account corrections for the Lorentz and polarization factors, and for absorption. All crystallographic calculations were carried out using the AREN programme system [25] using atomic scattering factors [26]. Crystal data, final positions and isotropic thermal parameters are listed in Table 2. The R factors and weighted R factors were respectively 0.06 and 0.057 (weighting of $1/2F_{min} + F + 2F^2/F_{max}$).

2.2.6. Infrared (IR) spectroscopy

Infrared spectra were recorded in the range 400–4000 cm^{-1} on samples dispersed in KBr using a DA8 FTIR instrument.

2.3. Cesium sorption

Radioactive ^{134}Cs was obtained by irradiating cesium nitrate in the neutron flux of the Orphee reactor using the facilities of the Pierre Süe Laboratory at Saclay. Sorption kinetics, sorption isotherms and maximum uptake were determined by batch experiments using the same procedure as described for $Cu_2Fe^{II}(CN)_6$ [13]. Three types of solutions were used: 0.1 M HNO_3, 0.2 M $LiBO_2$ (pH 8) in order to simulate solutions used in pressurized water nuclear reactors (PWR), and deionized water.

Table 2
Coordinates of atoms and thermal factor B in the P-1 triclinic crystal structure of $K_2CuFe(CN)_6$: $a = 0.6938(3)$ nm, $b = 0.6963(3)$ nm, $c = 0.7047(3)$ nm, $\alpha = 118.06(4)^\circ$, $\beta = 118.21(4)^\circ$ and $\gamma = 90.17(4)^\circ$

	x	y	z	B (nm)
K	0.811(1)	0.310(1)	0.539(2)	0.67(2)
Cu	0	0	0	0.47(2)
Fe	0.5	0.5	0	0.26(1)
C1	0.676(4)	0.286(4)	0.913(6)	0.43(4)
C2	0.265(5)	0.274(5)	0.915(6)	0.52(5)
C3	0.371(7)	0.312(6)	0.663(8)	0.71(8)
N1	0.792(5)	0.165(4)	−0.073(5)	0.54(5)
N2	0.132(7)	0.174(5)	−0.085(7)	0.78(7)
N3	0.345(13)	0.311(10)	0.487(13)	1.56(20)

The standard deviation on the last digit is indicated in parentheses.

3. Results

3.1. Synthesis

If solutions of potassium hexacyanoferrate (II) and copper salt with a K/Cu ratio close to 2 are poured simultaneously into water, the solution becomes pink, but no precipitate appears. Precipitation can be induced by adding a salt, such as an alkali chloride. This can be explained by the formation of a colloidal product, which then coagulates when the ionic strength of the solution is increased. If the K/Cu ratio is far from 2, or if one of the above solutions is poured into the other, precipitation occurs, but the quantities of solid separable by filtration are generally low. Although a variable but significant quantity of potassium is incorporated into the solid, the phase detected by X-ray diffraction is always $Cu^{II}_2Fe^{II}(CN)_6$, whose cubic structure was described in a previous study [13].

These results can explain the various K/Cu ratios in solids reported in the literature, when using such precipitation methods [16,30]. It is likely that the reported cubic structures do not correspond to a mixed $K_{2x}Cu^{II}_{2-x}Fe^{II}(CN)_6$ compound but to the presence of $Cu^{II}_2Fe^{II}(CN)_6$.

The local growth method is thus to be preferred and leads to a solid with a triclinic structure (see later). All the products used for sorption studies were so prepared. An overall yield of $\approx$75% is obtained, based on the amount of Cu. After washing and sieving, the yield for aggregates larger than 25 μm is $\approx$50%.

3.2. Influence of the washing procedure

By analyzing the chemical composition of the solid phases obtained in different syntheses after successive washing steps in water, we observed a decrease of the K/Cu ratio after each step, until an almost constant ratio. Before washing, the potassium content is high, probably due to the presence of potassium ions from the large excess of $K_4Fe^{II}(CN)_6$ in the solution. After the two first washing steps, the content of potassium falls drastically, as soluble potassium hexacyanoferrate is removed. The K/Cu ratio, at this stage, is close to 2 or slightly less than 2, depending on the synthesis. XRD patterns effectively show traces of $Cu_2Fe^{II}(CN)_6$, except when the K/Cu ratio is very close to 2. Further washing steps lead to a very slow decrease of the K/Cu ratio, which may be produced by a slight decomposition of $K_2CuFe^{II}(CN)_6$ into $Cu_2Fe^{II}(CN)_6$.

3.3. Characterization before sorption

3.3.1. Morphology

The size of the agglomerates prepared by local growth was between 25 and 500 μm (with $\approx$25% larger than 200 μm, $\approx$25% between 100 and 200 μm and $\approx$50% smaller than 100 μm). The mechanical strength of these aggregates, when they are shaken in aqueous solution (during stability or sorption experiments) is low. SEM images show aggregates (diameter from 5 to 50 μm) of porous platelets (Fig. 1a). At high resolution, these platelets appear to be formed of smaller particles leading to a general rugged aspect with, however, some particles of regular shape, which look like crystallites (Fig. 1b).

3.3.2. Chemical composition

Preparations led to a series of products with slightly variable chemical compositions (Table 1). The water content is derived from chemical analysis and thermogravimetric analyses. In each case, the composition is close to $K_2CuFe(CN)_6$, but the K/Cu atomic ratio is always below 2. In some compounds, there is a slight excess of cationic species, which might be explained by residual copper sulfate. XRD patterns confirm the presence of $Cu_2Fe^{II}(CN)_6$ and indicate the presence of other non-identified impurities, but $CuSO_4$ is never detected.

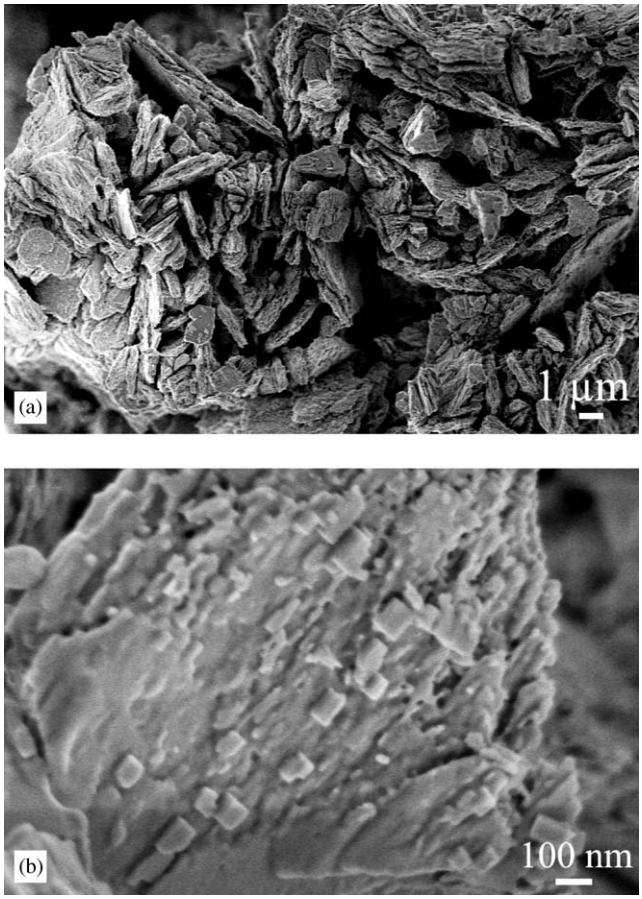

Fig. 1. (a, b) SEM images of $K_2CuFe(CN)_6$ prepared by the local growth method.

3.3.3. Specific surface area

The BET surface area was determined on the preparation coded Cu94.9. The surface area is low, 46 m^2/g, with a micropore volume of 0.042 m^3/g. Given the crystal structure (see below), structural porosity is unlikely and the surface area arises probably from inter-particle stacking.

3.3.4. Crystal structure before sorption

The powder diffraction patterns of $K_2CuFe(CN)_6$ powder show only a few lines and hence is difficult to index. However, intensities and reflections do not correspond to a cubic structure and are somewhat different from those published by Gellings [27] (ICDD 20.0875), corresponding to a tetragonal structure. The XRD patterns (Fig. 9) can be indexed by reference to the structure of single crystals. The width of the diffraction lines indicates the small size of the crystallites. Using the refinement of the whole pattern with the powdercell code [28] and the Williamson–Hall plot [29], the particle size was evaluated to 20–40 nm.

The structure obtained on single crystals can be fitted by a triclinic *P*-1 structure. It is presented in Fig. 2. Parameters of this structure are summarized in Table 2.

$K_2CuFe(CN)_6$ crystallises with a layered structure, with the planes developing along the crystallographic *ab* directions. Copper and iron are bridged through cyano groups, with carbon bonded to iron, and nitrogen to copper. This arrangement defines a square planar coordination environment for copper (r(Cu–N) = $2 \times 0.188(3)$, $2 \times 0.196(5)$ nm), while two additional CN groups complete the six-coordination sphere of iron (r(Fe–C) = $2 \times 0.179(4)$, $2 \times 0.191(4)$, $2 \times 0.198(3)$ nm). The negative charge on these polyanionic layers is balanced by interleaved potassium ions, the coordination shell of, which is made up of inter- and intra-layer carbon and nitrogen atoms. Distances between potassium and intra-layer carbon and nitrogen r(K—C2) and r(K—N2) (0.312(2) nm) are equal, suggesting interaction of potassium with the C≡N π-system. Short interatomic distances from interlayer carbon and nitrogen to potassium indicate non-bonding interactions that are probably responsible for the non-linearity of the Fe–C–N angle (<Fe–C≡N = 141°). The distance between two adjacent $(CuFe(CN)_6)_n^{2-}$ layers is 0.7 nm.

This structure is quite different from the *fcc* structure of Prussian blue-type observed for $Cu_2Fe(CN)_6$ [13]. The main differences are the layered structure with interleaved potassium ions, the non-linear –Fe–C–N–Cu– chains and the links not involving Cu atoms (Fe–C–N—K+). Two types of chemical reactivity can be predicted from this structure: exchange of K^+ ions with other cations, with kinetics that may be limited by the accessibility to the interplanar space between the –Fe–C–N–Cu layers, and eventually a reorganization of the structure via delamination. No structural water can be included in this framework, indicating that the measured water content is surface and zeolitic water.

3.3.5. Infra-red spectroscopy

The IR spectra of powdered $K_2CuFe(CN)_6$ after suspension in water and in dilute nitric acid are shown in Fig. 3. The dominant feature is the stretching vibration ν(C≡N) which is split into three components at 2074, 2085 and 2097 cm^{-1}. This splitting is also found in $K_4Fe(CN)_6$ and is a common feature for hexacyanoferrates. The relative intensities of these bands are slightly different in acid- and water-aged samples, but the positions are the same. Crystals of $K_2CuFe(CN)_6$ contain no water of hydration and, in agreement with this, the IR spectrum of Fig. 3 shows little evidence even of surface-bound water, unlike that of the acid-aged sample, which also shows the presence of nitrate groups (at 1385 cm^{-1}) and, possibly hydronium ions (at 1610 and 1660 cm^{-1}).

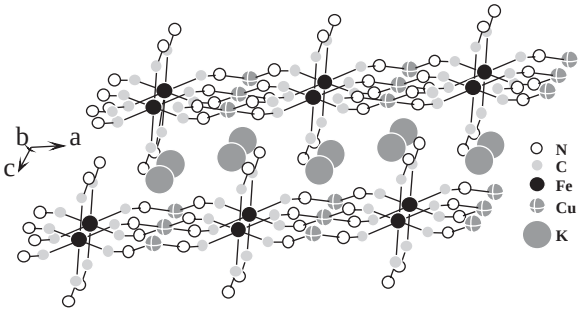

Fig. 2. Scheme of the crystal structure of $K_2CuFe(CN)_6$.

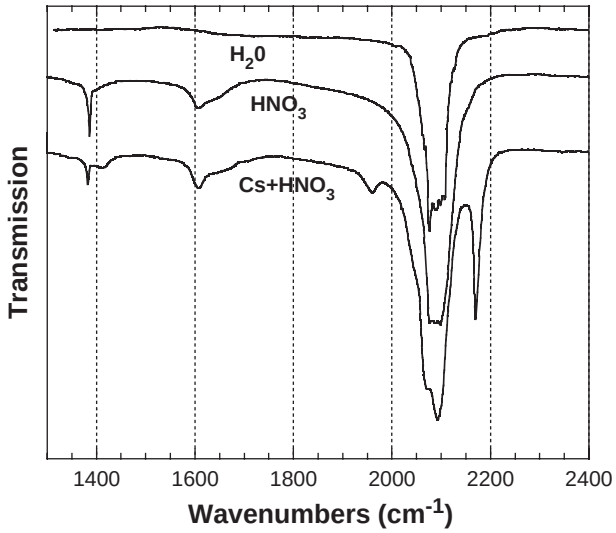

Fig. 3. Infra-red spectra of $K_2CuFe(CN)_6$ after contact with water, with a 0.1 M HNO_3 solution and with a 0.1 M HNO_3 solution containing Cs^+ ions.

3.4. Sorption of cesium

3.4.1. Maximum uptake

The highest observed uptakes are indicated in Table 3, together with some literature values. The highest reported value was observed in 3 N HNO_3 [30]. Somewhat different values can be obtained when starting from different preparations. Uptakes obtained in the present work in 0.1 M HNO_3 are close to reported values, but a marked discrepancy with literature values appears for the data obtained at pH 5–8. We note that, in our results, Cs uptake on $K_2CuFe(CN)_6$ is lower than on $Cu_2Fe(CN)_6$, whereas literature data report somewhat similar values for both sorbents. This discrepancy may be explained if, in previous studies, the solid is composed of a mixture of phases, with large quantities of $Cu_2Fe(CN)_6$, since, as noted above, it is difficult to obtain $K_2CuFe(CN)_6$ by conventional precipitation methods.

3.4.2. Sorption kinetics

The kinetics of sorption of cesium ions on $K_2CuFe(CN)_6$ in 0.1 M HNO_3 for an initial Cs/Fe atomic ratio of 2, is given in Fig. 4 as a function of time including all the measurements from 1 min to 6 months, and compared to the values obtained for $Cu_2Fe(CN)_6$ [13]. A $t^{1/2}$ time scale was chosen in order to expand the smallest time intervals. The results strongly depend on the sample and on the washing procedure used during the synthesis of the compounds. Preliminary experiments performed with an ill-defined compound (Cu93.24) show kinetics close to that of $Cu_2Fe(CN)_6$. X-ray diffraction indicates that this powder contains a non negligible amount of the $Cu_2Fe(CN)_6$ phase. With purer $K_2CuFe(CN)_6$, kinetics are slower and the quantities of cesium sorbed are lower than on $Cu_2Fe(CN)_6$ This is also the case for solutions of neutral pH containing lithium borate or not.

Sorption kinetics experiments were performed either directly, or using a solid pre-treated by stirring 17 h in 0.1 M HNO_3 or $LiBO_2$ solution before addition of the cesium salt. The uptake is faster when the sorbent is preconditioned in HNO_3 during the first minutes of experiments, but there is no difference after a few hours. This phenomenon is not observed in neutral pH solutions.

3.4.3. Sorption stoichiometry

A complete sorption balance including the determination of the sorbed quantity of cesium and the released quantities of elements constitutive of the solid was measured after 1 month of contact. Since no steady state of sorption was achieved even after 6 months, the variation of the sorbed quantity as a function of the initial concentration of cesium in the solution at 1 month of contact does not represent a true sorption isotherm. The results shown in Figs. 5 and 6 were obtained in deionized water and in 0.1 M HNO_3 solutions, respectively. In order to understand the stoichiometry of the process, we have indicated the variation of the quantity of sorbed cesium and the

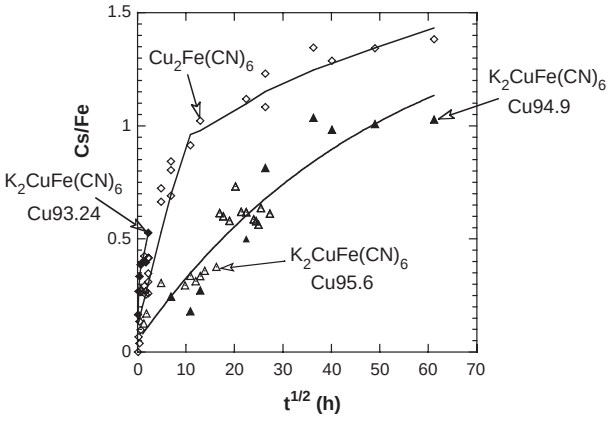

Fig. 4. Sorption kinetics of cesium on $K_2CuFe(CN)_6$ and $Cu_2Fe(CN)_6$ in a 0.1 M HNO_3 solution Variation of the sorbed quantity in atom per iron atom as a function of the square root of time.

Table 3
Maximum uptake of cesium ions[a] on various copper hexacyanoferrates (II)

Sorbent	5< pH <8	0.1 M HNO_3	Contact time	Reference
$K_{1.91}Cu^{II}_{1.05}[Fe^{II}(CN)_6]\cdot 3.4H_2O$[b]	0.4[a]	1.0	6 months	Present results
$K_{1.98}Cu^{II}_{1.18}[Fe^{II}(CN)_6]\cdot 1.9H_2O$[c]	0.4	1.3	1 month	Present results
$K_{1.91}Cu^{II}_{1.10}[Fe^{II}(CN)_6]\cdot 1.0H_2O$[d]	0.4	0.95	1 month	Present results
$K_{1.72}Cu^{II}_{1.09}Fe^{II}(CN)_6$		1.4[e]	24 h	[30]
$K_2Cu^{II}_3[Fe^{II}(CN)_6]_2\cdot 3.5H_2O$	0.82		96 h	[31]
$K_2Cu^{II}[Fe^{II}(CN)_6]\cdot 2H_2O$	1.02	1.13	72 h	[18]
$Cu^{II}_2[Fe^{II}(CN)_6]\cdot 16H_2O$	1.05	1.50	6 months	[13]

[a] In Cs atom per Fe atom.
[b] Code Cu93.24.
[c] Code Cu95.2.
[d] Code Cu95.3.
[e] 3 M HNO_3.

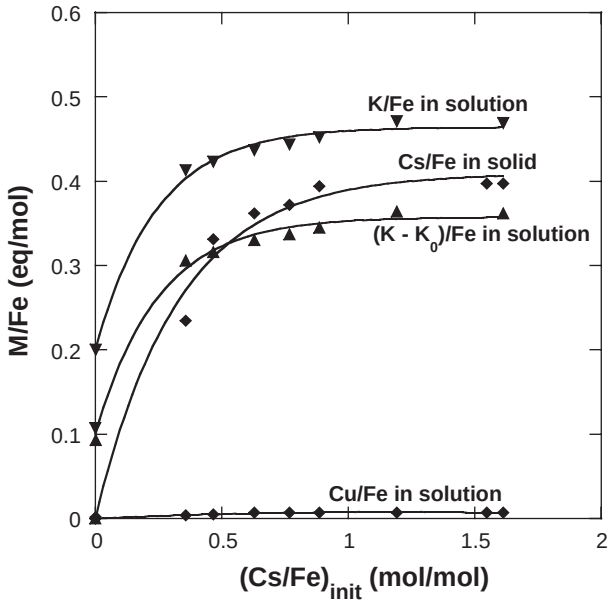

Fig. 5. Sorption stoichiometry of cesium on $K_2CuFe(CN)_6$ in deionized water. Variation of the Cs/Fe, K/Fe, $(K–K_0)$/Fe and Cu/Fe atomic ratios as a function of the Cs_i/Fe atomic ratio, where Cs and Fe represent the quantities of the corresponding elements in the solid, K and Cu the quantities of corresponding elements in the solution, K_0 the quantity of potassium in the solution without addition of cesium and Cs_i the initial quantity of cesium introduced in the solution.

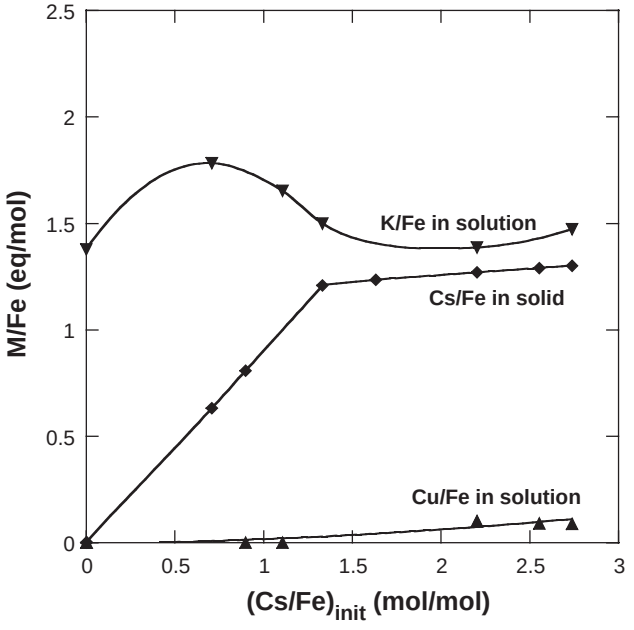

Fig. 6. Sorption stoichiometry of cesium on $K_2CuFe(CN)_6$ in 0.1 M HNO_3. Variation of the Cs/Fe, K/Fe and Cu/Fe atomic ratios as a function of the Cs_i/Fe atomic ratio, where Cs and Fe represent the quantities of the corresponding elements in the solid, K and Cu the quantities of potassium and copper in the solution and Cs_i the initial quantity of cesium introduced in the solution.

quantities of potassium and copper in solution. All these quantities are referred to 1 mol of iron in the solid.

In water (Fig. 5), for the solid Cu95.2, the quantity of sorbed cesium increases to a limit of ~0.4 mol/mol. The quantity of copper released into the solution is negligible. The quantity of released potassium is somewhat higher than the quantity of sorbed cesium. Even without cesium, ~0.1 mol/mol of potassium is released. This release can be interpreted by a partial exchange of K^+ with protons from the solution. Subtraction of the initial potassium release leads to values closer to the quantity of sorbed cesium, with a small deviation for the lowest and the highest cesium concentrations. However, the stoechiometry is close to 1/1, in favor of a Cs–K exchange, but the amount sorbed is low, if compared to the two "exchangeable" potassium atoms per iron atom. A small quantity of iron (~1%) was detected, the exact amount of which is difficult to measure, owing to the slow formation of precipitates in the filtered solutions.

In nitric acid solution, the process is quite different (Fig. 6). The "sorption isotherm" presents two parts: an almost linear part, with a slope close to one, indicating an almost quantitative sorption until ~1.2 mol/mol, followed by a plateau reaching ~1.3 mol/mol. Another feature is the high release of potassium, even without any addition of cesium (70% K released). This release may be attributed to an exchange of protons promoted by the high acidity of the solution, followed by a destruction of the solid. Infrared spectra (Fig. 3) show effectively the possible presence of hydronium ions. With an increase in the amount of cesium, the release of potassium first increases and then decreases, but is always higher than the quantity of sorbed cesium. There is a high deficit of measured cationic charge in the solid, which may be compensated by the presence of protons. At higher cesium concentrations, this deficit decreases and the positive charge approaches 4. Copper release is low, however slightly higher than in neutral solution for the highest cesium quantities. Quantities of iron released are small but higher than in neutral solutions.

3.5. Evolution of the solid

3.5.1. General aspect and composition

After 1 day in the presence of cesium and $K_2CuFe(CN)_6$, neutral solutions turn pink, while nitric solutions turn pale yellow. A few days after filtration, the acid solutions become blue, with probably the formation of Prussian blue. Neutral solutions are more stable, but turbid. The solid after filtration and washing presents a heterogeneous aspect, showing a pink powder with a few darker particles in neutral medium, a yellow powder with black particles in acid medium, dark particles represent a small part of the whole solid.

It was possible to separate the dark particles from the powder using tweezers. Each of these types of solids was analyzed by neutron activation analysis. The results are compared in Table 4 to the mean concentrations in the solid deduced from the analysis of the filtrates. In the case of sorption in deionized water, washing decreases

Table 4
Composition of the solid after a contact time of 1 month in deionized water and 0.1 M HNO_3 solutions with cesium: mole ratios in the solid before washing and in the two types of particles after washing

Solution	Initial Cs/Fe[a]	K/Cu		Dark particles	Mean solid	Cs/Cu		M/Fe[b]
		Overall[c]	Powder			Powder	Dark particles	
Water	0.36	1.31	1.23	0.77	0.25	0.28	0.39	4.2
Water	0.77	1.28	1.19	0.85	0.26	0.31	0.42	4.2
Water	1.19	1.25	1.47	0.80	0.27	0.24	0.43	4.15
Water	1.61	1.26	1.14	0.93		0.34	0.42	4.2
HNO_3	0.90	0.06	0.05	0.05	0.61	0.49	0.43	3.15
HNO_3	1.10	0.11	0.17	0.06	0.63	0.56	0.58	3.2
HNO_3	2.20	0.16	0.23	0.14	1.15	0.69	0.71	3.9
HNO_3	2.75	0.22	0.22	0.12	1.12	0.73	0.74	3.95

Starting sorbent: $K_{1.98}Cu^{II}_{1.18}[Fe^{II}(CN)_6]\cdot 1.9H_2O$ (Cu95.2).
[a] Initial atomic Cs/Fe ratio in the solution before sorption.
[b] (Cs + K + Cu)/Fe ratio in equivalent per Fe atom, in the mean solid before washing.
[c] Analysis of the total solid before washing.

the potassium content of the solid. Cesium is more concentrated in the dark particles. In the case of sorption in nitric acid, washing decreases the cesium content of the solid, but this element is uniformally distributed between the two types of solids. As already pointed out, a large quantity of potassium has been transferred to the liquid phase, but the total cation charge is close to 4, for the highest Cs contents.

3.5.2. SEM observation after Cs sorption

SEM observations were performed on solids after 1 month of contact with cesium in a 0.1 M nitric solution. On product Cu95.3 with a final composition Cs/Fe ~ 0.3, K/Fe ~ 0.2, we observed the pink powder and the dark particles separately. At low magnification, the aggregates have the same appearance as that of the starting solid. At higher magnification, the platelets, instead of being porous and rugged, appear with well-defined surfaces and contours (Fig. 7a). The dark particles appear to be formed of more compact aggregates of well-defined particles (Fig. 7b). Sample Cu95.2 with a final composition Cs/Fe ~ 1, K/Fe ~ 0.2, is constituted either of zones of geometrically defined platelets or particles (Fig. 8a), or smaller particles separated by pores (Fig. 8b). It is clear, that in nitric solutions, sorption of cesium lead to a complete modification of the morphology of the solid.

3.5.3. Infrared spectroscopy

The most striking observation (Fig. 3) when $K_2CuFe(CN)_6$ is dispersed for long periods in acidic solutions containing cesium ion is the appearance of an additional, intense absorption band at high frequency (2178 cm^{-1}). As described above, four of the cyano groups are bound within the layers to copper and iron, while the other two cyano groups are involved in non-bonding interaction with interlayer potassium ions. It may be inferred from the IR spectrum that the non-bonding interactions are disrupted when potassium ion is lost to an acidic solution containing cesium, and that any interaction of the corresponding CN groups with cesium is weaker in character.

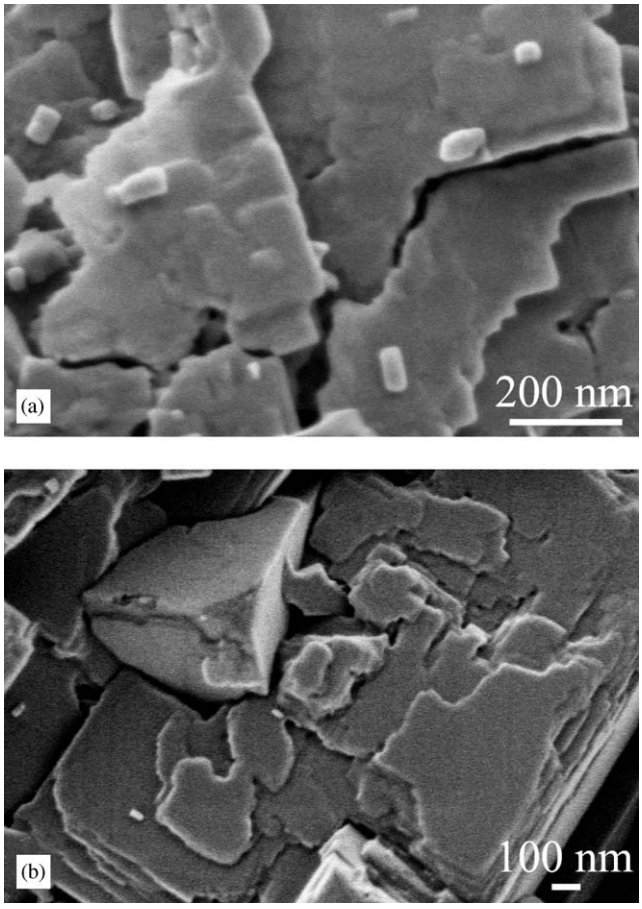

Fig. 7. (a, b) SEM images of $K_2CuFe(CN)_6$ (Cu95.3) after cesium sorption in 0.1 M HNO_3.

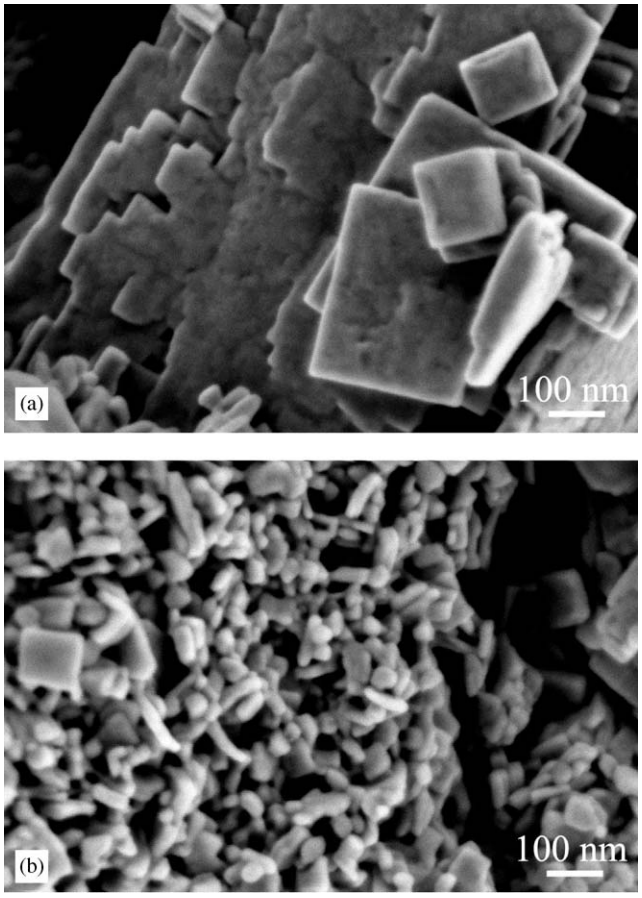

Fig. 8. (a, b) SEM images of $K_2CuFe(CN)_6$ (Cu95.2) after cesium sorption in 0.1 M HNO_3.

Another possibility however, is the partial oxidation of iron to Fe^{III}, the absorption band at 2178 cm^{-1} being attributable to $\nu(Fe^{III}–CN–Cu^{II})$, and that at 2105 cm^{-1} to $\nu(Fe^{II}–CN–Cu^{II})$ [32]. Additional evidence is provided from the Mössbauer spectrum of the material recovered after sorption of cesium is complex, with two resonances of equal intensity and having chemical shifts −0.08 and −0.15 mm/s (quadrupole splittings of 0.08 and 0.87 mm/s), that can be interpreted as resulting from the presence of Fe^{II} and Fe^{III}, respectively [32].

Features at 1385, 1416, 1610 and 1660 cm^{-1} in the infrared spectrum also show the presence of nitrate ion, water and, probably, protonated water species.

3.5.4. Crystal structure after sorption

X-ray diffraction analyses were performed on powders after 6 months of contact with deionized water, $LiBO_2$ solutions and 0.1 HNO_3 solutions, without or with cesium.

After contact with water, the structure is unchanged (Fig. 9), with however a modification of line ratios indicating an increase of the concentration of the traces of $Cu_2Fe(CN)_6$ phase, which contributes to the shoulder at 35.9° 2Θ, to the shifting of the line at 18°, and to the modification of the group of lines at 25°. In presence of cesium ions the structure remains unchanged, with a further modification of the line ratios.

In $LiBO_2$ solutions, in presence or not of cesium ions, the structure of $K_2CuFe(CN)_6$ is also unchanged, with also a modification of line ratios.

In 0.1 N HNO_3 solution, the initial structure is destroyed (Fig. 10). The main lines can be identified as those of $Cu_2Fe(CN)_6 \cdot xH_2O$, with traces of Prussian blue. In the presence of cesium ions, neither $K_2CuFe(CN)_6$ nor $Cu_2Fe(CN)_6 \cdot xH_2O$ phases are observed. The diffractogram presents several common

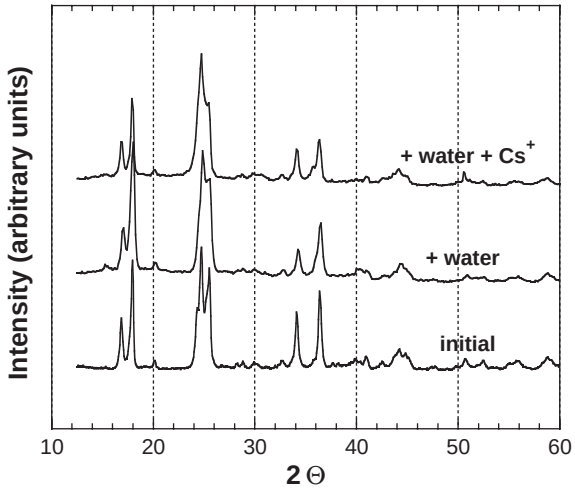

Fig. 9. X-ray diffraction patterns of initial $K_2CuFe(CN)_6$ (Cu94.9), of the same solid treated by desionized water and of the same solid treated by deionized water containing cesium (Cs/Fe = 0.22 in the solid).

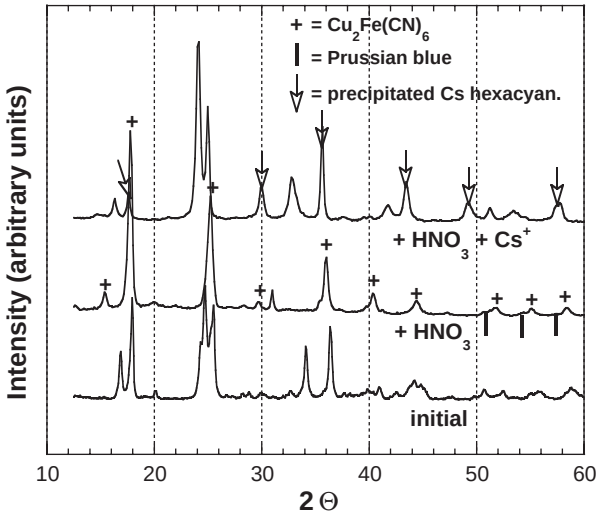

Fig. 10. X-ray diffraction patterns of initial $K_2CuFe(CN)_6$ (Cu94.9), of the same solid treated by 0.1 M HNO_3 solutions and of the same solid treated by HNO_3 solutions containing cesium (Cs/Fe = 0.9 in the solid). Positions of main diffraction lines of $Cu_2Fe(CN)_6$, Prussian blue and precipitated cesium hexacyanoferrate are indicated.

lines with that observed in the case of $Cu_2Fe(CN)_6 \cdot x$-H_2O in the presence of cesium in 0.1 HNO_3 solution [13] and in the case of a cesium-copper hexacyanoferrate precipitated according to Kuznetsov [33]. This author has proposed a cubic structure with a $Cs_2Cu_3[Fe(CN)_6]_2$ composition for this precipitate, while we have measured a composition close to $Cs_2CuFe(CN)_6$ [13]. This result indicates that such compound is one of the products formed from both $K_2CuFe(CN)_6$ nor $Cu_2Fe(CN)_6$ in presence of cesium ions in nitric acid solutions. Other products with unknown compositions and structures are also formed.

4. Discussion

4.1. Preparation, stability and crystal structure

Several authors have described the preparation of compounds with various K/Cu ratios with the hypothesis of definite compounds and/or solid solutions between $K_2CuFe(CN)_6$ and $Cu_2Fe(CN)_6$ [10]. These hypotheses are the basis for the interpretation of the results obtained by electrochemical measurements [19–21]. A structure with a three-dimensional network and channels through which potassium and other ions can move, was proposed, with reversible exchange of alkali metal ions.

We could never obtain powders with compositions close to $K_2CuFe(CN)_6$, nor phases which could be interpreted as $K_{2x}Cu_{2-x}Fe(CN)_6$ solid solutions [11 and present study], by mixing potassium hexacyanoferrate and copper salt solutions in various proportions. The obtained separable phase is cubic $Cu_2Fe(CN)_6$.

The way to produce $K_2CuFe(CN)_6$ (crystal sizes 20–40 nm) was the local growth method [22–24], but the triclinic *P*-1 structure of this phase is quite different from the cubic structure found in many hexacyanoferrates such as Prussian blue, $Cu_2Fe(CN)_6$ and nickel hexacyanoferrates [8–9]. It should be noticed that by simply broadening the lines of the $K_2CuFe(CN)_6$ structure, it was possible to simulate the "tetragonal structure" described by Gellings [27]. The presence of potassium seems not to be possible in the cubic symmetry and leads to non linear –Fe–C–N–Cu– chains and to a lamellar structure, which can be at the origin of the ability of this compound for cation exchange.

It seems therefore that a separable powder of $K_2CuFe(CN)_6$ or $K_{2x}Cu_{2-x}Fe(CN)_6$ cannot be obtained by conventional precipitation by mixing solutions with a stoechiometric K/Cu ratio or not. This method leads preferentially to cubic $Cu_2Fe(CN)_6$. However, the presence of colloidal phases containing both potassium and copper is not excluded, but these phases are removed by filtration and washing. As a consequence, the existence of cubic copper hexacyanoferrates containing variable concentrations of alkali metals and which are often the basis of the interpretation of electrochemical measurements [19–21], is questionable.

In addition, $K_2CuFe(CN)_6$ seems to have a limited stability, since small quantities of $Cu_2Fe(CN)_6$ are often present as a trace impurity and since, in 0.1 M nitric acid solution, an almost total transformation into $Cu_2Fe(CN)_6$, with traces of Prussian blue is observed.

4.2. Sorption mechanisms

By comparing the results of sorption stoechiometry (Fig. 5) and X-ray diffraction (Fig. 9), it is clear that in neutral pH (deionized water and $LiBO_2$) sorption proceeds by an exchange of potassium by cesium without modifying the crystal structure. Thus, as predicted, a cation exchange process can occur in this crystal structure, but potassium is far from being entirely exchanged, since, even for the longest durations of contact and the highest cesium concentration, the exchange is limited to $\sim$0.4 mol/mol.

It was possible to simulate the X-ray patterns of $Cs_xK_{2-x}CuFe(CN)_6$ using the FullProf software [34] for various Cs/K ratios (Fig. 11). Substitution of cesium has a marked effect on the ratio of the diffraction lines at 16.3 and 17.8° 2Θ and this evolution also appears in the experimental patterns. However, a complete quantitative comparison between experimental and simulated patterns is difficult, due to the presence of $Cu_2Fe(CN)_6$ phase and differences in line widths.

Fig. 5 shows that, in neutral solutions, the Cs/K exchange slightly deviates from a 1/1 stoechiometry since a little more potassium is released into solution

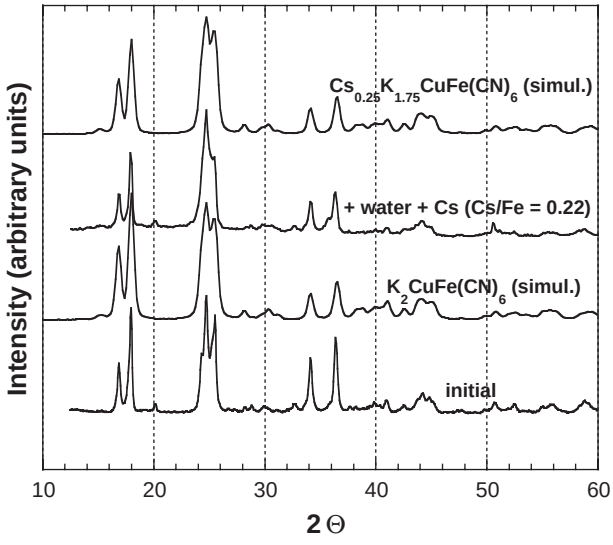

Fig. 11. Numerical simulation of X-ray diffraction patterns of $K_2CuFe(CN)_6$ and $Cs_{0.25}K_{1.75}CuFe(CN)_6$, with comparison to the experimental patterns of initial $K_2CuFe(CN)_6$ and of the same solid treated by deionized water containing cesium (Cs/Fe = 0.22).

than cesium is sorbed and a certain quantity of potassium is released, even in the absence of cesium. This may result from a partial substitution of potassium by protons or from the formation of $Cu_2Fe(CN)_6$, leading to the formation of a small quantity of other phases.

The sorption mechanism is quite different in acid solutions. Even without cesium, the initial structure is destroyed (Fig. 7, 8, 10) and a large proportion of potassium ($\sim$1.4 mol/mol) is released into solution (Fig. 6). This transformation leads essentially to $Cu_2Fe(CN)_6$ with traces of Prussian blue and, possibly other phases. In the presence of cesium, the initial structure is also destroyed (Fig. 10), $Cu_2Fe(CN)_6$ does not appear in the diffraction pattern, but one of the new phase(s) formed is the same as one of the phases formed from $Cu_2Fe(CN)_6$ in presence of cesium. The variation of the quantity of released potassium as a function of sorbed cesium (Fig. 6), which indicates an increase and then a decrease of the measured cation charge in the solid, may be interpreted as the formation of an intermediate protonated hexacyanoferrate. For the highest cesium concentrations, the total cation charge again approaches 4. These facts support the hypothesis of the presence of H^+ in the hexacyanoferrate complex, with the possible affinity range $K^+ < H^+ < Cs^+$. The maximum sorbed quantity ($\sim$1.3 mol/mol) is larger in acid medium than in neutral solutions.

One of the most striking results of this study is the difference of behavior between neutral and acid solutions. The only common effect in both types of solutions is the absence of release of copper from the solid into the solution. The sorption mechanism is quite different from that observed on $Cu_2Fe(CN)_6$, where, after a first step in which we observed sorption of ion pairs, the initial structure is destroyed with a release of copper into solution, both in neutral and acid media [13]. In the present case, the initial structure is maintained in neutral solution. The sorption kinetics and the final products are also different. The sorbed quantity is higher in $Cu_2Fe(CN)_6$, both in neutral and acid solutions (Table 3). It is very likely that earlier studies which indicated large quantities of sorbed cesium, were not performed with pure potassium-copper hexacyanoferrates (II).

The present study confirms our earlier results that the sorption mechanisms strongly depend on the composition and structure of hexacynoferrates and that a true ion exchange occurs only with specific products and specific experimental conditions. Structures with alkali metal ions included in zeolitic cavities as in rhombohedral $M^I_2Zn_3[Fe(CN)_6]_2$ (M^I = Na, K, Cs) or in interlamellar space as in triclinic $K_2CuFe(CN)_6$, are favorable for cation exchange. However, fast diffusion in the zeolitic structure of $M^I_2Zn_3[Fe(CN)_6]_2$ leads to a fast and total exchange, while, in $K_2CuFe(CN)_6$, the diffusion is much slower in the inter-lamellar space, leading to slow sorption kinetics and prevents total exchange even after several months of contact. The question is why, in acidic media, a cation exchange process does not take place. In fact, it probably takes place, but, in presence of a large concentration of H^+ in solution, protons are exchanged preferentially to cesium, leading to the above-noted apparent deficit in the cationic charge, since the content of protons cannot be measured in the solid. Protonated hexacyanoferrates such as $H_2CuFe(CN)_6$ are unstable and decompose into more stable compounds, $Cu_2Fe(CN)_6$ and Prussian blue in absence of cesium or other compounds including cesium, when this ion is present.

Absence of an exchange process is not contradictory to the ability to remove cesium from aqueous solutions. In the case of $Cu_2Fe(CN)_6$, which does not present exchange properties, the maximum sorbed quantity is larger than in $K_2CuFe(CN)_6$ and than in all other hexacyanoferrates we have studied. Although limited quantities can be retained by a surface process or by the insertion of ion pairs, sorption of large quantities of cesium without ion exchange lead to the destruction of the initial structure and the formation of new solid phases.

However, the ability to retain large quantities of cesium without ion exchange depends on the crystal structure. As an example, $Cu_2Fe(CN)_6$, because of its microporosity and ability to absorb molecules and ion pairs, is then able to transform completely into new phases including large quantities of cesium. On the contrary, $Cu_3[Fe(CN)_6]_2$ which does not have this ability, retains only small quantities by a surface process [13]. $Zn_2Fe(CN)_6$ which has a trigonal compact structure, retains cesium, but with a slow process controlled by the formation of a shell of new phase on the surface of the initial solid phase [12].

Sorption mechanisms have a consequence on the use of hexacyanoferrates for the decontamination of liquid radioactive wastes. The main favorable factors for the use in column are the sorption kinetics, and the chemical and mechanical stability. The sorption capacity is not a very important factor for radioactive cesium, since the maximum permissible radioactivity of the column is achieved very long before the chemical capacity is reached. A sorption process with a phase transformation is not favorable, since it leads to a modification of the solid morphology and flow rate in the column. $K_2CuFe(CN)_6$ seems not to be the best sorbing material in spite of the ion exchange process in neutral solutions, because of the slow kinetics. In that sense, $M^I_2Zn_3[Fe(CN)_6]_2$ are good compounds, because, in neutral solutions, they show a fast ion exchange process, but they have a certain unstability in aqueous solutions. $Cu_2Fe(CN)_6$, on the contrary, is one of the most stable hexacyanoferrates.

Another point to consider is the long-term storage of the solid as a waste after its use as a sorbent for cesium. In the present study, we have seen that the evolution of the solid is far from being complete after a period of 6 months. Structural changes can last for very long times and may be hazardous for long time storage. Other factors common to hexacyanoferrate powders are the small size of particles and a certain mechanical unstability, which render their industrial use in columns difficult.

A good way to overcome these difficulties is to limit the quantity of hexacyanoferrate and to deposit it on an inert support, such as a composite material formed of silica and of an organic polymer [35,36]. Experiments with copper hexacyanoferrate prepared by such a way showed a very good stability in column and very high sorption rates.

5. Conclusion

This study, based on several different and complementary investigation methods, showed that mixed potassium-copper hexacyanoferrates (II) of definite composition and separable by filtration cannot be obtained by conventional precipitation in aqueous solution, in disagreement with previous data. This technique leads to solids with a $Cu_2Fe(CN)_6$ structure. A powder of composition $K_2CuFe(CN)_6$ can be obtained by the local growth method [22–24] or by growth in a gel. This compound has a triclinic structure, which was described for the first time in the present work. This crystal structure is made up of non linear –Fe–C–N–Cu– chains which form a puckered layered network, and so differs completely from the fcc Prussian blue-type observed for $Cu_2Fe(CN)_6$ and several other hexacyanoferrates.

This work confirms our previous studies, which have shown that the sorption mechanisms strongly depend on the composition and structure of the hexacyanoferrate, together with the composition of the aqueous solution, leading either to an ion exchange, or to the formation of new solid phases. Again, it is clear that a good knowledge of sorption mechanisms can be achieved only by working on well defined compounds, which, in turn, necessitates long efforts of synthesis and characterization. In the present case, cesium is sorbed by a cation exchange mechanism in neutral solutions and by decomposition–precipitation process in acid solutions. A long-term evolution of the solids takes place in both cases. For application to the decontamination of liquid radioactive wastes, complementary packaging strategies are required.

References

[1] G.B. Barton, J.L. Helpworth, E.D. McClanahan Jr, R.L. Moore, H.H. Van Tuyl, Ind. Eng. Chem. 50 (1958) 212.
[2] H. Loewenschuss, Radioact. Waste Manage 2 (1982) 327.
[3] E.W. Hooper, AERE-R-12338,1987; AERE-G 4421, 1988.
[4] D.O. Campbell, D.D. Lee, T.A. Dillow, J.L. Collins, IAEA-TecDoc-675, 1992, p. 85.
[5] P.A. Haas, Sep. Sci. Technol. 28 (1993) 2479.
[6] J. Lehto, L. Szirtes, Radiat. Phys. Chem. 43 (1994) 261.
[7] Proceedings of the First Hanford Separation Science Workshop, July 23–25, 1991, PNL-SA-21775, 1991.
[8] C. Loos-Neskovic, M. Fedoroff, E. Garnier, P. Gravereau, Talanta 31 (1984) 1133.
[9] C. Loos-Neskovic, M. Fedoroff, E. Garnier, Talanta 36 (1989) 749.
[10] S. Ayrault, C. Loos-Neskovic, M. Fedoroff, E. Garnier, Tatanta 41 (1994) 1435.
[11] S. Ayrault, C. Loos-Neskovic, M. Fedoroff, E. Garnier, D.J. Jones, Talanta 42 (1995) 1581.
[12] C. Loos-Neskovic, M. Fedoroff, Solvent Extr. Ion Exchange 7 (1989) 131.
[13] S. Ayrault, B. Jimenez, E. Garnier, M. Fedoroff, D. Jones, C. Loos-Neskovic, J. Solid State Chem. 141 (1998) 475.
[14] E. Garnier, P. Gravereau, A. Hardy, Acta Crystallogr. B 38 (1982) 1401.
[15] A.K. Jain, R.P. Singh, C. Bala, J. Radioanal. Chem. 75 (1982) 85.
[16] E.F.T. Lee, M. Streat, J. Chem. Technol. Biotechnol. 33A (1983) 333.
[17] M.T. Ganzerli Valentini, R. Stella, M. Cola, J. Radioanal. Nucl. Chem. 102 (1986) 99.
[18] P. Nielsen, B. Dresow, H.C. Heinrich, Z. Naturf., Chem. Sci. 42B (1987) 1451.
[19] L.M. Siperko, T. Kuwana, J. Electrochem. Soc. 130 (1983) 396.
[20] D. Engel, E. W. Grabner. Z. Phys. Chem. 160 (1988) 151.
[21] D. Schwudke, R. Stösser, F. Scholz, Electrochem. Commun. 2 (2000) 301.
[22] M. Fedoroff, C. Loos-Neskovic, French Patent 84-12139, 1984.
[23] C. Loos-Neskovic, S. Abousahl, M. Fedoroff, J. Mater. Sci. 25 (1990) 677.
[24] S. Abousahl, C. Loos-Neskovic, M. Fedoroff, J. Cryst. Growth 137 (1994) 569.
[25] V.I. Andrianov, Sov. Phys. Crystallogr. 32 (1987) 130.
[26] J.A. Ibers, W.C. Hanilton, International Tables for X-ray Crystallography, Vol. IV, The Kynoch Press, Birmingham, 1974.
[27] P.J. Gellings, Z. Phys. Chem. 54 (1967) 296.
[28] W. Kraus, G. Nolze, International Union of Crystallography, CPD Newsletter 20, May–August 1998.
[29] G.K. Williamson, W.H. Hall, Acta Metall. 1 (1954) 22.
[30] R. Pfrepper, G. Pfrepper, ZfI. Mitteilungen 116 (1986) 43.
[31] E.F.T. Lee, M. Streat, J. Chem. Technol. Biotechnol. 33A (1983) 80.
[32] C.W. Ng, J. Ding, Y. Shi, L.M. Gan, J. Phys. Chem. Solids 62 (2001) 767.
[33] V.G. Kuznetsov, Z.V. Popova, G.B. Seifer, Zh. Neorg. Khim. 15 (1970) 2105.
[34] J. Rodriguez-Carvajal, T. Roisnel, FullProf.98 and WinPLOTR NewWindows 95/NT Applications for Diffraction, International Union of Crystallography, CPD Newsletter 20, May–August 1998.
[35] C. Loos-Neskovic, C. Vidal-Madjar, B. Jimenez, A. Pantazaki, V. Federici, A. Tamborini, M. Fedoroff, E. Persidou, Radiochim. Acta 85 (1999) 143.
[36] C. Loos-Neskovic, C. Vidal-Madjar, J. Dulieu, A. Pantazaki, French Patent FR 97 08723 (July 9 1997), Intern. Patent WO 99 02 255.